Comparing SWIPT Techniques for Zero-Energy RIS

Dimitrios Tyrovolas*†, Vasilis K. Papanikolaou*, Sotiris A. Tegos*, Yue Xiao‡,
Panagiotis D. Diamantoulakis*, Sotiris Ioannidis†, Christos Liaskos§, George K. Karagiannidis*¶
*Dept. of Electrical and Computer Engineering, Aristotle University of Thessaloniki, Thessaloniki, Greece
e-mail: {tyrovolas, vpapanikk, tegosoti, padiaman, geokarag}@auth.gr
† Dept. of Electrical and Computer Engineering, Technical University of Chania, Chania, Greece.
e-mail: sotiris@ece.tuc.gr
‡ School of Information Science and Technology, Southwest Jiaotong University, Chengdu, China.
e-mail: xiaoyue@swjtu.edu.cn
§Computer Science Engineering Department, University of Ioannina, Ioannina,
and Foundation for Research and Technology Hellas (FORTH), Greece.
e-mail: cliaskos@ics.forth.gr
¶Cyber Security Systems and Applied AI Research Center, Lebanese American University (LAU), Lebanon

2023 IEEE International Conference on Communications Workshops (ICC Workshops) | 979-8-3503-3307-7/23/$31.00 ©2023 IEEE | DOI: 10.1109/ICCWORKSHOPS57953.2023.10283652

***Abstract*—Providing enhanced quality of service (QoS) to support demanding applications in the most energy-efficient way has been identified as a primary objective of future 6G networks. Towards this direction, the concept of programmable wireless environments (PWEs) has emerged, wherein extremely high QoS can be ensured by controlling the wireless propagation through reconfigurable intelligent surfaces (RIS). To meet the demands of 6G networks in terms of energy efficiency, in this paper, zero-energy RISs (ZERISs) are introduced, which harvest the required amount of energy for their operation and then contribute to the PWE conversion. More specifically, we investigate the performance of a ZERIS-assisted communication system in terms of joint energy-data rate outage probability, which quantifies the trade-off between the harvested energy and information transmission, for three distinct simultaneous wireless information and power transfer (SWIPT) methods are investigated, namely power splitting, time switching, and element splitting. Finally, simulation results validate the derived analysis, leading to useful insights for the ZERIS-assisted network regarding which energy harvesting method achieves better performance in terms of joint energy-data rate outage probability.**

***Index Terms*—Wireless Power Transfer (WPT), Reconfigurable Intelligent Surfaces (RIS), Zero-Energy Devices (ZEDs), Performance Analysis**

I. Introduction

Recently, academia and industry are focusing on 6G networks, which are expected to provide superior quality of service (QoS) compared to 5G and satisfy futuristic services and applications in the most energy-efficient way [1]. Towards this direction, a novel wireless communication paradigm denoted as programmable wireless environments (PWEs) has emerged, which strives to constitute the wireless propagation phenomenon into a software-defined process, to achieve truly ubiquitous connectivity [2]. To realize this, it is needed to coat the environment's planar objects with metasurfaces with well-defined networking and programming interfaces. Reconfigurable intelligent surfaces (RISs) constitute a popular metasurface technology, built upon the phase shifter paradigm. RISs can alter the power, direction, polarization, and phase of any impinging wave through their reflecting elements in a nearly-passive way. In this way, deployed RISs can be dynamically orchestrated to realize custom end-to-end propagation routes, enhance the wireless channels' quality, and even realize futuristic applications such as sensing and extended reality through RF-imaging [3]–[5].

Deployment-wise, RISs should be ideally self-powered via energy harvesting (EH). This direction is inspired by the wireless power transfer (WPT) paradigm, a green networking technology that allows for self-powered devices and network components–also known as zero-energy devices (ZEDs)–which operate by harvesting energy from RF signals [2], [6], [7]. Related studies have recently considered the challenge of transforming RISs into ZEDs, denoted in this paper as *zero-energy RISs (ZERISs)*, in order to create completely green and extremely easily deployable PWEs. A self-sustainable RIS was proposed in [8] to enhance a WPT system using an absorb-then-reflect scheme, without considering information transmission, while in [9], self-powered RISs have been utilized in wireless-powered communication networks. Finally, in [10], the sum-rate maximizing problem was investigated in a self-sustainable RIS-aided system, where information users (i.e., communicating clients) and energy users (i.e., WPT clients) are served separately. Nevertheless, none of the aforementioned works has deduced which is the most appropriate simultaneous wireless information and power transfer (SWIPT) method to enable ZERISs.

In the present analysis, we investigate three major SWIPT methods for the operation of a ZERIS, denoted as: i) *power splitting (PS)*, i.e., tunable absorption and beam manipulation per ZERIS element, ii) *time switching (TS)*, i.e., alternating between absorption and beam manipulation over time per element, and iii) *element splitting (ES)*, i.e., distinct absorption or beam manipulation per element. These methods differ with each other, since the number of reflecting elements that require energy varies for each method, e.g., in TS the reflecting elements consume power for a portion of time. Specifically, we consider a point-to-point communication system, where a ZERIS harvests the required amount of energy for its

operation, while also assisting the information transmission through its beam manipulation functionality. To this direction, we first derive the required ZERIS operation energy for each of the examined methods, and then we provide closed-form expressions for the joint energy-data rate outage probability, which quantifies the trade-off between the harvested energy and information transmission for all the examined SWIPT methods.

II. System Model

We consider the downlink of a communication network with perfectly-acquired channel state information, consisting of a single-antenna base station (BS) that serves an assigned ground node (GN) via a ZERIS, which steers its impinging radiation towards the GN. In more detail, due to the harshness of the propagation environment, a BS selects a ZERIS with N reflecting elements to serve a nearby single-antenna GN with which it shares a pure LoS link [11]. Finally, to enable the ZERIS operation, it needs to harvest energy through its absorption functionality. Hence, it is important to explore the most appropriate way to perform the absorption functionality, without degrading the network's reliability.

A. Power splitting

PS is based on the signal power division into two energy streams, the EH stream, and the information transmission stream. Specifically, the tunable PS factor $\rho \in [0,1]$ determines the power of the EH stream, while the information transmission stream is proportional to $1-\rho$. Thus, the received signal for the PS case can be expressed as

$$y_{\rm PS}(t) = \sqrt{\ell P_t (1-\rho) G} \sum_{i=1}^{N} |h_{1i}||h_{2i}| e^{j\phi_i} x(t) + n(t), \quad (1)$$

where P_t is the transmit power, $G = G_t G_r$ is the product of the antenna gains, and N the number of reflecting elements. Furthermore, $\ell = \ell_1 \ell_2$ is the end-to-end link's path loss and it is equal to the product of the path losses of the BS-ZERIS and the ZERIS-GN links that are given as

$$\ell_u = C_0 d_u^{-a_u}, \quad (2)$$

where $u \in \{1,2\}$, while C_0 is the path loss at the reference distance d_0, d_1 is the BS-ZERIS distance, d_2 is the ZERIS-GN distance, and a_1, a_2 denote the path loss exponents for the BS-ZERIS and ZERIS-GN channels, respectively. Moreover, $|h_{1i}|$ and $|h_{2i}|$ are the gains of the channels between the BS and the i-th reflecting element and between the i-th reflecting element and the GN, respectively, where $|h_{1i}|$ is assumed to be a random variable (RV) following Nakagami-m distribution with shape parameter m_1, and scale parameter Ω_1, while $|h_{2i}| = 1$ due to the pure LoS nature of the i-th reflecting element-GN channel. In what follows, the term $|h_{2i}|$ is omitted for brevity. Finally, $\phi_i = \omega_i + \arg(h_{1i}) + \arg(h_{2i})$, where ω_i is the phase shift induced by the i-th reflecting element, $\arg(h_{1i})$ is the phase of h_{1i}, and $\arg(h_{2i})$ is the phase of h_{2i} which is equal to $\frac{2\pi d_2}{\lambda}$. It should be highlighted that the PS factor ρ is assumed to be equal for all the reflecting elements. Therefore, the instantaneous rate when the PS method is applied and the ZERIS is perfectly configured for the beam-steering functionality, i.e., ω_i is set equal to $-\arg(h_{1i}) - \arg(h_{2i})$, can be expressed as

$$R_{\rm PS} = \log_2 \left(1 + \gamma_t G \ell (1-\rho) \left| \sum_{i=1}^{N} |h_{1i}| \right|^2 \right), \quad (3)$$

where $\gamma_t = \frac{P_t}{P_n}$ is the transmit SNR with P_n being the noise power.

In order to utilize a ZERIS the required amount of energy for its operation needs to be expressed. Therefore, considering that N reflecting elements will be configured to simultaneously absorb power and steer the impinging wave towards the user according to the PS method, the required amount of energy can be expressed as

$$E_{\rm PS} = T (N P_e + P_{\rm circ}), \quad (4)$$

where T is the symbol time duration, P_e is the consumption of each reflecting element and $P_{\rm circ}$ is the consumption of the ZERIS controller that sets the configuration of each element. It should be mentioned that, in this work, it is assumed that only the reflecting elements operating for information transmission consume power. Thus, considering a linear EH model [12], the harvested energy when the PS model is applied is given as

$$Q_{\rm PS} = T \rho \zeta P_t G_t \ell_1 \left| \sum_{i=1}^{N} h_{1i} e^{j\omega_i} \right|^2. \quad (5)$$

Moreover, to maximize the amount of harvested energy, the phase shift term ω_i should be equal to $-\arg(h_{1i})$, to achieve the maximum channel gain. However, considering that in PS the ZERIS is configured to perform the beam-steering functionality, the channel gain for the harvested energy is equal to $\left| \sum_{i=1}^{N} |h_{1i}| e^{j \frac{2\pi d_2}{\lambda}} \right|$, where after some algebraic manipulations, it can be rewritten as $\left| \sum_{i=1}^{N} |h_{1i}| \right|$. Thus, the amount of harvested energy when PS is applied can be rewritten as

$$Q_{\rm PS} = T \rho \zeta P_t G_t \ell_1 \left| \sum_{i=1}^{N} |h_{1i}| \right|^2. \quad (6)$$

B. Time switching

In the TS case, the received signal is used solely for EH or receiving information during specific time periods. Specifically, T is divided into two time intervals, where within the first time interval, i.e., $[0, \tau T]$, the ZERIS is configured for EH, while within the second time interval, i.e., $(\tau T, T]$, the RIS is configured for information transmission, where $\tau \in [0,1]$ is the portion of the symbol time T where the reflecting elements are configured for EH. Thus, the received signal for the TS case is expressed as

$$y_{\rm TS}(t) = \begin{cases} 0, & 0 \le t \le \tau T \\ \sqrt{\ell P_t G} \sum_{i=1}^{N} |h_{1i}| e^{j\phi_i} x(t) + n(t), & \tau T < t \le T. \end{cases} \quad (7)$$

Therefore, the instantaneous rate at the receiver when the TS method is applied can be expressed as

$$R_{\mathrm{TS}} = (1-\tau)\log_2\left(1+\gamma_t G\ell\left|\sum_{i=1}^{N}|h_{1i}|\right|^2\right). \tag{8}$$

Accordingly to the PS case, we need to define the energy that needs to be harvested via the TS method. Hence, considering that all reflecting elements will be configured for information transmission only for a specific amount of time, then the required energy for the TS case is given as

$$E_{\mathrm{TS}} = T\left((1-\tau)NP_e + P_{\mathrm{circ}}\right). \tag{9}$$

Thus, in order to maximize the absorbed energy within the EH time interval, the phase shift term of each reflecting element is set as $\omega_i = -\arg(h_{1i})$. Therefore, the harvested energy for the linear EH model can be expressed as

$$Q_{\mathrm{TS}} = T\left(\tau\zeta P_t G_t \ell_1\left|\sum_{i=1}^{N}|h_{1i}|\right|^2\right). \tag{10}$$

C. Element splitting

Aside from the PS and the TS methods, the large number of reflecting elements enables a ZERIS to harvest energy through the ES method. In more detail, for the ES method, N_1 reflecting elements are configured for EH, while the rest of them are configured for information transmission. Therefore, the received signal for the ES case can be expressed as

$$y_{\mathrm{ES}}(t) = \sqrt{\ell P_t G}\sum_{i=1}^{N_2}|h_{1i}|e^{j\phi_i}x(t) + n(t), \tag{11}$$

where N_2 is the number of reflecting elements contributing to the information transmission, through the beam-steering functionality. Thus, the instantaneous rate at the GN when the ES method is applied is given as

$$R_{\mathrm{ES}} = \log_2\left(1+\gamma_t G\ell\left|\sum_{j=1}^{N_2}|h_{1i}|\right|^2\right), \tag{12}$$

Finally, considering the number of reflecting elements that participate in the beam-steering functionality, the required energy for a ZERIS that performs ES is given as

$$E_{\mathrm{ES}} = T\left(N_2 P_e + P_{\mathrm{circ}}\right). \tag{13}$$

To this end, the harvested energy can be expressed as

$$Q_{\mathrm{ES}} = T\zeta P_t G_t \ell_1\left|\sum_{i=1}^{N_1}|h_{1i}|\right|^2. \tag{14}$$

It should be highlighted that T is assumed to be equal to 1, therefore for the rest of the paper it is omitted for brevity.

III. Joint Energy–Data Rate Outage Probability

As aforementioned, a ZERIS needs to harvest the appropriate amount of energy in order to perform its functionalities, e.g., beam-steering. Thus, to evaluate the reliability of a communication system based on a ZERIS performing the beam-steering functionality, we calculate the *joint energy-data rate outage probability* which is defined as the union of the energy outage event, i.e., the ZERIS has not harvested the required amount of energy for its operation, and the data rate outage event, i.e., the received SNR is lower than a predefined SNR threshold. Therefore, in this section, we present analytic expressions for the joint energy-data rate outage probability of the examined EH methods, which can be expressed as [12]

$$P_j^q = \Pr\left(Q_q \le E_q \ \cup \ R_q \le \log_2(1+\gamma_{\mathrm{thr}})\right), \tag{15}$$

where Q_q is the amount of harvested energy, R_q is the instantaneous rate at the GN, $q \in \{\mathrm{PS}, \mathrm{TS}, \mathrm{ES}\}$ indicates which EH method is applied, and γ_{thr} is a predefined SNR threshold.

Proposition 1: The joint energy-data rate outage probability for the PS protocol can be approximated as

$$P_j^{\mathrm{PS}} \approx \frac{1}{\Gamma(k_{\mathrm{PS}})}\gamma\left(k_{\mathrm{PS}}, \frac{\max\left(w_{\mathrm{PS}}, \sqrt{\frac{\gamma_{\mathrm{thr}}}{\gamma_t G\ell(1-\rho)}}\right)}{\theta_{\mathrm{PS}}}\right), \tag{16}$$

where

$$k_{\mathrm{PS}} = \frac{N\left(\frac{\Gamma(m_1+\frac{1}{2})}{m_1}\right)^2}{m_1 - \left(\frac{\Gamma(m_1+\frac{1}{2})}{m_1}\right)^2}, \tag{17}$$

$$\theta_{\mathrm{PS}} = \frac{\sqrt{m_1\Omega_1}\left(1-\frac{1}{m_1}\left(\frac{\Gamma(m_1+\frac{1}{2})}{\Gamma(m_1)}\right)^2\right)}{\frac{\Gamma(m_1+\frac{1}{2})}{\Gamma(m_1)}}, \tag{18}$$

and

$$w_{\mathrm{PS}} = \sqrt{\frac{NP_n + P_{\mathrm{circ}}}{\rho\zeta P_t G_t \ell_1}}, \tag{19}$$

where $\zeta \in [0,1]$ is the energy conversion efficiency.

Proof: By taking into account (3) and (6), the joint energy-data rate outage probability for the PS method can be expressed as

$$P_j^{\mathrm{PS}} = \Pr\left(\rho\zeta P_t G_t \ell_1\left|\sum_{i=1}^{N}h_{1i}\right|^2 \le NP_n + P_{\mathrm{circ}} \ \cup \ \log_2\left(1+\gamma_t G\ell(1-\rho)\left|\sum_{i=1}^{N}|h_{1i}|\right|^2\right) \le \log_2(1+\gamma_{\mathrm{thr}})\right), \tag{20}$$

which after algebraic manipulations can be rewritten as

$$P_j^{\mathrm{PS}} = \Pr\left(\left|\sum_{i=1}^{N}\left|h_{1i}\right|\right| \le w_{\mathrm{PS}} \cup \left|\sum_{i=1}^{N}|h_{1i}|\right| \le \sqrt{\frac{\gamma_{\mathrm{thr}}}{\gamma_t G\ell(1-\rho)}}\right). \tag{21}$$

It can be observed that $Z = \left|\sum_{i=1}^{N}|h_{1i}|\right|$ is upper bounded in both events. Specifically, the union of these events occurs

when Z is lower than the maximum of these upper bounds. Hence, P_j^{PS} can be further expressed as

$$P_j^{\mathrm{PS}} = \Pr\left(Z \leq \max\left(\sqrt{\frac{NP_n + P_{\mathrm{circ}}}{\rho\zeta P_t G_t \ell_1}}, \sqrt{\frac{\gamma_{\mathrm{thr}}}{\gamma_t G\ell\,(1-\rho)}} \right) \right). \tag{22}$$

Considering the large number of configured reflecting elements, i.e., $N \geq 50$, by invoking the moment-matching technique Z can be tightly approximated by a Gamma-distributed RV with scale and shape parameters $k_{\mathrm{PS}} = \frac{\mathbb{E}^2[Z]}{\mathrm{Var}[Z]}$ and $\theta_{\mathrm{PS}} = \frac{\mathrm{Var}[Z]}{\mathbb{E}[Z]}$, respectively, where $\mathbb{E}[\cdot]$ denotes expectation and $\mathrm{Var}[\cdot]$ denotes variance. Hence, we need to calculate the mean value and the variance of Z which can be expressed, respectively, as

$$\mathbb{E}[Z] = \mathbb{E}\left[\left| \sum_{i=1}^{N} |h_{1i}| \right| \right] = N\mathbb{E}\left[|h_{1i}|\right] = N\sqrt{\frac{\Omega_1}{m_1}} \frac{\Gamma(m_1 + \frac{1}{2})}{\Gamma(m_1)} \tag{23}$$

and

$$\begin{aligned} \mathrm{Var}[Z] &= \mathrm{Var}\left[\left| \sum_{i=1}^{N} |h_{1i}| \right| \right] = N\mathrm{Var}\left[|h_{1i}|\right] = \\ &= N\Omega_1 \left(1 - \frac{1}{m_1} \left(\frac{\Gamma(m_1 + \frac{1}{2})}{\Gamma(m_1)} \right)^2 \right). \end{aligned} \tag{24}$$

Hence, after the calculation of k_{PS} and θ_{PS}, by utilizing the cumulative density function (CDF) of Gamma distribution which is equal to

$$F_g(x) = \frac{\gamma(k_{\mathrm{PS}}, \frac{x}{\theta_{\mathrm{PS}}})}{\Gamma(k_{\mathrm{PS}})}, \tag{25}$$

then P_j^{PS} is derived, which concludes the proof. ∎

In contrast with the PS method where the ZERIS simultaneously performs the beam-steering with the absorption functionality, when the TS protocol is applied, the ZERIS is configured for energy absorption until it harvests the required amount of energy, and then all its elements are reconfigured to serve the data transmission via beam-steering. Thus, in the following proposition, we provide the joint energy-data rate outage probability for the case where the TS method is applied

Proposition 2: The joint energy-data rate outage probability when the TS method is applied can be approximated as

$$P_j^{\mathrm{TS}} \approx \frac{1}{\Gamma(k_{\mathrm{TS}})} \gamma \left(k_{\mathrm{TS}}, \frac{\max\left(w_{\mathrm{TS}}, \sqrt{\frac{(1+\gamma_{\mathrm{thr}})^{\frac{1}{1-\tau}} - 1}{\gamma_t G\ell}} \right)}{\theta_{\mathrm{TS}}} \right), \tag{26}$$

where $k_{\mathrm{TS}} = k_{\mathrm{PS}}$, $\theta_{\mathrm{TS}} = \theta_{\mathrm{PS}}$, and by taking into account the linear EH model, then w_{TS} is given by

$$w_{\mathrm{TS}} = \sqrt{\frac{(1-\tau)\,NP_n + P_{\mathrm{circ}}}{\tau\zeta P_t G_t \ell_1}}. \tag{27}$$

Proof: Following a similar process with the PS method, to calculate the joint energy-data rate probability for the presented communication system when the TS method is applied, we need the amount of harvested energy Q_{TS}, as well as the instantaneous rate R_{TS}. Thus, by substituting (8), and (10) in (15) and after some algebraic manipulations, the joint energy-data rate outage probability can be written as

$$P_j^{\mathrm{TS}} = \Pr\left(Z \leq w_{\mathrm{TS}} \cup Z \leq \sqrt{\frac{(1+\gamma_{\mathrm{thr}})^{\frac{1}{1-\tau}} - 1}{\gamma_t G\ell N^2}} \right). \tag{28}$$

Finally, by following the moment-matching technique as presented in *Proposition 1*, the joint energy-data rate outage probability can be derived as in (26), which concludes the proof. ∎

In addition to the PS and the TS methods, a ZERIS can also operate by dividing its reflecting elements into two parts: N_1 reflecting elements performing the absorption functionality to assist in the EH, meaning that their induced phase shift is set as $\omega_i = -\arg(h_{1i})$, and N_2 reflecting elements performing the beam-steering functionality for information transmission, meaning that their induced phase shift is set as $\omega_i = -\arg(h_{1i}) - \arg(h_{2i})$. To this end, in the following proposition, the joint energy-data rate outage probability for the ES case is derived.

Proposition 3: The joint energy-data rate outage probability when the ES method is applied can be approximated as in (29) at the top of the next page, where

$$m_{\mathrm{es}}(N_i) = \frac{(\Omega_{\mathrm{es}}(N_i))^2}{f(N_i) - (\Omega_{\mathrm{es}}(N_i))^2}, \tag{31}$$

$$\Omega_{\mathrm{es}}(N_i) = N_i \left(E[{R_1}^2] + (N_i - 1)E^2[R_1] \right), \tag{32}$$

with $N_i \in \{N_1, N_2\}$, $E[{R_1}^n] = \frac{\Gamma(m_1 + n/2)}{\Gamma(m_1)} \left(\frac{\Omega_1}{m_1} \right)^{n/2}$, $f(N_i)$ is given in (30) at the top of the next page and

$$w_{\mathrm{ES}} = \sqrt{\frac{N_2 P_n + P_{\mathrm{circ}}}{\zeta P_t G_t \ell_1}}. \tag{33}$$

Proof: Similarly with the PS and the TS methods, to calculate the joint energy-data rate outage probability for the ES case, we need the amount of harvested energy as well as the instantaneous rate at the GN. Thus, by substituting (12) and (14) in (15), the joint energy-data rate outage probability can be expressed as

$$P_j^{\mathrm{ES}} = \Pr\left(\left| \sum_{i=1}^{N_1} |h_{1i}| \right| \leq w_{\mathrm{ES}} \ \cup \ \left| \sum_{j=1}^{N_2} |h_{1j}| \right| \leq \sqrt{\frac{\gamma_{\mathrm{thr}}}{\gamma_t G\ell}} \right). \tag{34}$$

As it can be observed, the RVs that are upper bounded in (34) are different and independent of each other, due to the fact that different reflecting elements perform the absorption and the beam-steering functionality. Therefore, the above probability can be rewritten as

$$\begin{aligned} P_j^{\mathrm{ES}} = &\Pr\left(\left| \sum_{i=1}^{N_1} |h_{1i}| \right| \leq w_{\mathrm{ES}} \right) + \Pr\left(\left| \sum_{j=1}^{N_2} |h_{1j}| \right| \leq \sqrt{\frac{\gamma_{\mathrm{thr}}}{\gamma_t G\ell}} \right) \\ &- \Pr\left(\left| \sum_{i=1}^{N_1} |h_{1i}| \right| \leq w_{\mathrm{ES}} \right) \Pr\left(\left| \sum_{j=1}^{N_2} |h_{1j}| \right| \leq \sqrt{\frac{\gamma_{\mathrm{thr}}}{\gamma_t G\ell}} \right). \end{aligned} \tag{35}$$

$$P_j^{\mathrm{ES}} \approx \frac{\gamma\left(m_{\mathrm{es}}(N_1), \frac{m_{\mathrm{es}}(N_1)}{\Omega_{\mathrm{es}}(N_1)}(w_{\mathrm{ES}}^{v})^2\right)}{\Gamma(m_{\mathrm{es}}(N_1))} + \frac{\gamma\left(m_{\mathrm{es}}(N_2), \frac{m_{\mathrm{es}}(N_2)}{\Omega_{\mathrm{es}}(N_2)}\frac{\gamma_{\mathrm{thr}}}{\gamma_t G\ell}\right)}{\Gamma(m_{\mathrm{es}}(N_2))} - \left(\frac{\gamma\left(m_{\mathrm{es}}(N_1), \frac{m_{\mathrm{es}}(N_1)}{\Omega_{\mathrm{es}}(N_1)}(w_{\mathrm{ES}}^{v})^2\right)}{\Gamma(m_{\mathrm{es}}(N_1))}\right)\left(\frac{\gamma\left(m_{\mathrm{es}}(N_2), \frac{m_{\mathrm{es}}(N_2)}{\Omega_{\mathrm{es}}(N_2)}\frac{\gamma_{\mathrm{thr}}}{\gamma_t G\ell}\right)}{\Gamma(m_{\mathrm{es}}(N_2))}\right), \tag{29}$$

$$f(N_i) = N_i\Big(E[{R_1}^4] + 4(N_i-1)E[{R_1}^3]E[{R_1}^2] + 3(N_i-1)E^2[{R_1}^2] + 6(N_i-1)(N_i-2)E[{R_1}^2]E^2[R_1] + (N_i-1)(N_i-2)(N_i-3)E^4[R_1]\Big), \tag{30}$$

Considering that N_1 and N_2 are not necessarily large, by taking into account the approximation presented in [13] the sum of N_i independent and identically distributed Nakagami-m RVs can be approximated by a Nakagami-m RV with shape parameter $m_{\mathrm{es}}(N_i)$ and scale parameter $\Omega_{\mathrm{es}}(N_i)$, respectively. Finally, considering the CDF of Nakagami-m distribution which is equal to

$$F_n(x) = \frac{\gamma\left(m_{\mathrm{es}}(N_i), \frac{m_{\mathrm{es}}(N_i)x^2}{\Omega_{\mathrm{es}}(N_i)}\right)}{\Gamma\left(m_{\mathrm{es}}(N_i)\right)}, \tag{36}$$

then (29) is derived, which concludes the proof. ■

IV. Numerical Results

In this section, Monte Carlo simulations with 10^6 realizations are presented to numerically validate the provided analysis. The downlink performance of a ZERIS-assisted network is investigated, where the ZERIS harvests energy and steers the impinging waves towards a GN to establish communication between the BS and the GN. In the presented figures, the BS-ZERIS distance d_1 is set equal to 30 m, while the ZERIS-GN distance d_2 is set equal to 15 m. Furthermore, the noise power is assumed to be $P_n = -100$ dB, C_0 is set equal to -32 dB, the antenna gains G_t and G_r are assumed to be equal to 1, and the path loss exponents for the BS-ZERIS and ZERIS-GN links are set as $a_1 = 2.2$ and $a_2 = 2$, respectively. Moreover, unless otherwise stated, the transmit power P_t is set at 1 W, the shape and scale parameters of h_{1i} are assumed to be equal to $m_1 = 3$ and $\Omega_1 = 1$, respectively, while the SNR threshold γ_{thr} is assumed to be 20 dB. Finally, regarding the ZERIS consumption and the EH model we assume that the energy conversion efficiency is $\zeta = 0.75$, the consumption of each reflecting element is set as $P_e = 2$ μW and the ZERIS controller consumption is set equal to $P_{\mathrm{circ}} = 50$ mW [14].

In Fig. 1, the joint energy-data rate outage probability is illustrated when the PS method is utilized. In more detail, the outage probability is presented with regards to the PS factor ρ for various values of N, i.e., the number of ZERIS reflecting elements. Firstly, the analytical and the numerical results are clearly in agreement, validating the derived analysis. On top of that, it can be observed that a larger number of reflecting elements is critical in reducing the required portion of power for EH. Also, interestingly, the outage probability is seen to get close to unity again for large values of ρ, something that is attributed to the fact that as $\rho \to 1$, then $\mathrm{SNR} \to 0$ causing a data rate outage phenomenon.

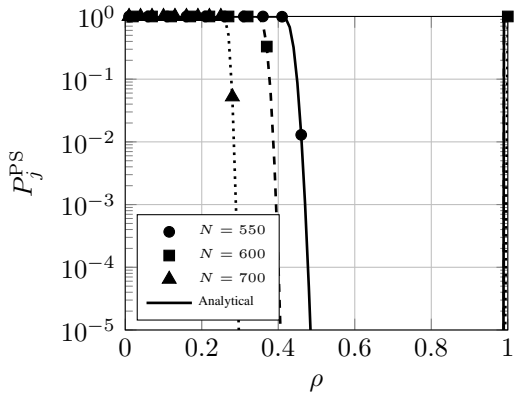

Fig. 1. Joint energy-data rate outage probability versus ρ for PS.

In Figs. 2 and 3, a similar behavior can be observed. For the TS method, there exists a more narrow set of τ values that can lead to low outage probabilities, which is especially true when $N = 550$. In the case of TS, the optimal value of τ is close to 0.5, whereas in the case of ES, the optimal value of $\frac{N_1}{N}$ is around 0.8. In both of these cases and more clearly than when PS is utilized, when either τ or $\frac{N_1}{N}$ tends to 1, the outage probability also tends to unity.

Finally, in Fig. 4, the three methods are presented for $N = 500$ with regards to the BS's transmit power. It should be mentioned that the values of $\rho = 0.96$, $\tau = 0.47$, and $\frac{N_1}{N} = 0.818$ are the values that present the optimal joint energy-data rate outage probability for the case where $N = 500$. As it can be observed, the PS method outperforms the rest, requiring around half of the transmitted power that TS requires to achieve a low enough joint outage probability. ES achieves intermediate performance amongst the other methods. Once again, it is clear that the analytical results are validated through the Monte Carlo simulations. On top of that, it should be noted that the steep descent these curves showcase is attributed to the almost deterministic nature of the wireless channel, which is the primary purpose of the ZERIS in the context of PWEs.

V. Conclusions

In this paper, we investigated three different EH methods that can be applied by a ZERIS, in terms of the joint energy-data rate outage probability, to conclude which one enables

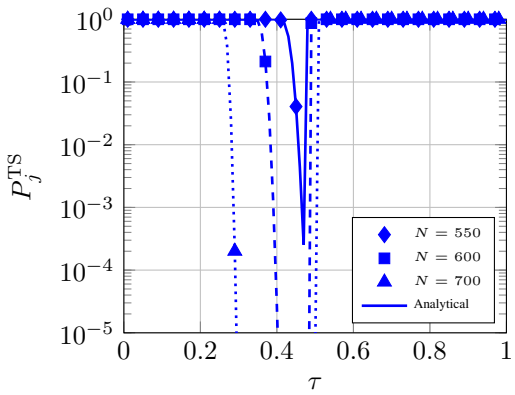

Fig. 2. Joint energy-data rate outage probability versus τ for TS.

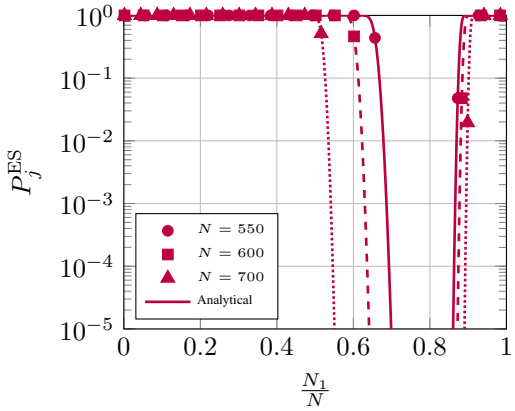

Fig. 3. Joint energy-data rate outage probability versus $\frac{N_1}{N}$ for ES.

reliable communications with as less transmit power as possible. Specifically, the PS method outperforms the rest, requiring around half of the transmitted power that TS requires, whereas the ES method achieves intermediate performance amongst the other methods. Our future directions include the case where the ZERIS-GN link is affected by small-scale fading phenomena, as well as additional techniques to further reduce the utilized power.

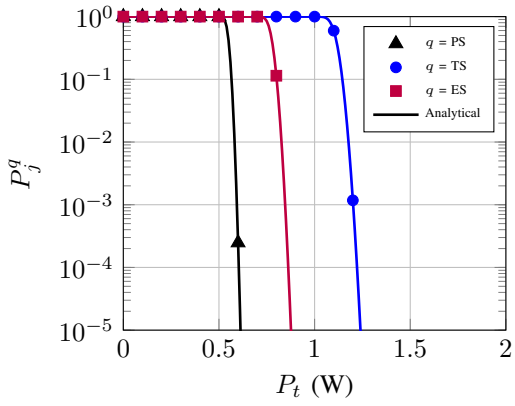

Fig. 4. Joint energy-data rate outage probability versus transmit power P_t.

VI. Acknowledgments

This work has been funded by the European Union's Horizon 2020 research and innovation programme under Grant Agreement No. 952690 (CYRENE), and the FORTH Synergy Grant 2022 'WISAR'. The work of V. K. Papanikolaou was co-financed by Greece and the European Union (European Social Fund-ESF) through the Operational Programme "Human Resources Development, Education and Lifelong Learning" in the context of the Act "Enhancing Human Resources Research Potential by undertaking a Doctoral Research" Sub-action 2: IKY Scholarship Programme for PhD candidates in the Greek Universities. The work of Yue Xiao was supported by National NSFC 62201477 and Sichuan Youth Fund Project 2023NSFSC1374.

References

[1] Z. Zhang, Y. Xiao, Z. Ma, M. Xiao, Z. Ding, X. Lei, G. K. Karagiannidis, and P. Fan, "6G wireless networks: Vision, requirements, architecture, and key technologies," *IEEE Veh. Technol. Mag.*, vol. 14, no. 3, pp. 28–41, 2019.

[2] C. Liaskos, A. Tsioliaridou, S. Nie, A. Pitsillides, S. Ioannidis, and I. F. Akyildiz, "On the network-layer modeling and configuration of programmable wireless environments," *IEEE ACM Trans Netw.*, vol. 27, no. 4, pp. 1696–1713, 2019.

[3] D. Tyrovolas, S. A. Tegos, E. C. Dimitriadou-Panidou, P. D. Diamantoulakis, C. K. Liaskos, and G. K. Karagiannidis, "Performance analysis of cascaded reconfigurable intelligent surface networks," *IEEE Wireless Commun. Lett.*, vol. 11, no. 9, pp. 1855–1859, 2022.

[4] S. P. Chepuri, N. Shlezinger, F. Liu, G. C. Alexandropoulos, S. Buzzi, and Y. C. Eldar, "Integrated sensing and communications with reconfigurable intelligent surfaces," 2022. [Online]. Available: https://arxiv.org/abs/2211.01003

[5] C. Liaskos *et al.*, "XR-RF imaging enabled by software-defined metasurfaces and machine learning: Foundational vision, technologies and challenges," *IEEE Access*, pp. 1–1, 2022.

[6] S. Bi, Y. Zeng, and R. Zhang, "Wireless powered communication networks: an overview," *IEEE Wirel. Commun.*, vol. 23, no. 2, pp. 10–18, 2016.

[7] N. A. Mitsiou, V. K. Papanikolaou, P. D. Diamantoulakis, and G. K. Karagiannidis, "Energy-aware optimization of zero-energy device networks," *IEEE Commun. Lett.*, vol. 26, no. 4, pp. 858–862, 2022.

[8] Y. Cheng, W. Peng, and T. Jiang, "Self-sustainable RIS aided wireless power transfer scheme," *IEEE Trans. Veh. Technol.*, pp. 1–12, 2022.

[9] H. Xie, B. Gu, D. Li, Z. Lin, and Y. Xu, "Gain without pain: Recycling reflected energy from wireless powered RIS-aided communications," 2022. [Online]. Available: https://arxiv.org/abs/2209.13100

[10] Y. Pan, K. Wang, C. Pan, H. Zhu, and J. Wang, "Self-sustainable reconfigurable intelligent surface aided simultaneous terahertz information and power transfer (STIPT)," *IEEE Trans. Wirel. Commun.*, vol. 21, no. 7, pp. 5420–5434, 2022.

[11] C. You, B. Zheng, W. Mei, and R. Zhang, "How to deploy intelligent reflecting surfaces in wireless network: BS-Side, User-Side, or Both Sides?" *J. Commn. Net.*, vol. 7, no. 1, pp. 1–10, 2022.

[12] S. A. Tegos, P. D. Diamantoulakis, K. N. Pappi, P. C. Sofotasios, S. Muhaidat, and G. K. Karagiannidis, "Toward efficient integration of information and energy reception," *IEEE Trans. Commun.*, vol. 67, no. 9, pp. 6572–6585, 2019.

[13] J. C. S. S. Filho and M. D. Yacoub, "Nakagami-m approximation to the sum of M non-identical independent Nakagami-m variates," *Electronics Letters*, vol. 40, no. 15, p. 951, Jan. 2004.

[14] D. Tyrovolas, P.-V. Mekikis, S. A. Tegos, P. D. Diamantoulakis, C. K. Liaskos, and G. K. Karagiannidis, "Energy-aware design of UAV-mounted RIS networks for IoT data collection," *IEEE Trans. Commun.*, pp. 1–1, 2022.